

Measurements of isolated prompt photons in pp collisions with the ATLAS detector

Martín Tripijana* on behalf of the ATLAS Collaboration

Instituto de Física de La Plata (UNLP-CONICET)

E-mail: Martin.Tripijana@cern.ch

ATLAS has measured the production cross section of events with one and two isolated prompt photons in the final state, in proton-proton collisions at a center-of-mass energy $\sqrt{s} = 7$ TeV. The results presented here are based on the full data set collected in 2010 with the ATLAS detector at the Large Hadron Collider. Photon candidates are identified by combining information from the calorimeters and from the inner tracker. Residual background in the selected sample is estimated from data, based on the observed distribution of the transverse isolation energy in a narrow cone around the photon candidate. The results are compared to predictions from next-to-leading order perturbative QCD calculations.

*The 2011 Europhysics Conference on High Energy Physics-HEP 2011,
July 21-27, 2011
Grenoble, Rhône-Alpes France*

*Speaker.



The production of prompt (di-)photons at hadron colliders occurs mainly through parton hard scattering, thus providing a handle for testing perturbative QCD (pQCD) predictions [1]. The dominant production mechanism of single prompt photon at Large Hadron Collider (LHC) energies is $qg \rightarrow q\gamma$, which can be particularly useful to constrain the gluon density in protons [2]. In the case of prompt di-photons, the production may occur through quark-antiquark annihilation, $q\bar{q} \rightarrow \gamma\gamma$, or via gluon-gluon interaction, $gg \rightarrow \gamma\gamma$. The latter, mediated by a quark box diagram, becomes comparable to the LO contribution given the large gluon flux at the LHC.

Here we present the two measurements of the inclusive isolated prompt photon production cross section, $d\sigma/dE_T$, based on $\sim 0.88\text{pb}^{-1}$ [3] and $\sim 35\text{pb}^{-1}$ [4] of data collected during 2010. The recent measurement of the di-photon production cross section [5] using 37pb^{-1} of 2010 data is also reported.

The ATLAS detector is described in Ref. [6]. Events are triggered by a single [3, 4] or double [5] high-level photon trigger. Events in which the calorimeters or the inner detector are not fully operational, or show data quality problems, are discarded. A primary vertex consistent with the beam spot position and with at least three associated tracks is required, to reduce non-collision backgrounds.

Photons are reconstructed from clusters of energy deposits in the electromagnetic calorimeter (ECAL) [7]. A careful treatment is applied in case of one or more tracks associated to the cluster, to separate photons converting in front of the ECAL from true isolated e^\pm . The residual electron background is estimated from the $e^\pm\gamma$ pairs with an invariant mass under the Z-peak.

The main photon background comes from hadronic jets. Most of these jets are suppressed by requiring little energy deposited in the hadronic calorimeter and a narrow shower profile in the middle layer of the ECAL. The remaining background comprises mostly collimated photon pairs from energetic π^0 and η decays. It can be reduced by using the high granularity in η of the first layer of the ECAL, by looking for two maxima or a shower width not compatible with that of a single photon. Further suppression is achieved by means of the isolation energy, E_T^{iso} , defined as the transverse energy surrounding the photon in a cone of radius $R = 0.4$ ¹. The contribution to E_T^{iso} from the photon itself and from the underlying activity in the event² is subtracted. A photon is defined as isolated if $E_T^{iso} < 3\text{GeV}$, which corresponds to a parton/particle-level isolation requirement of 4 GeV [3].

The background contamination in the selected (di-)photon sample is estimated, and then subtracted in a data-driven way. For the prompt photon analysis, a counting method is applied, with the signal and control (*sidebands*) regions defined by the shower identification and the isolation criteria [3, 4]. An extended version of this method is used in the di-photon analysis [5], where the signal and control regions are also defined for the second p_T -leading photon.

The measured prompt photon differential cross section, as a function of E_T is shown in Fig. 1. A good agreement is observed between the two measurements [3, 4] and with the theoretical NLO predictions from JETPHOX [9] for $E_T > 35\text{ GeV}$. Below, where the theory overestimates the data, more accurate predictions and a better modeling of the fragmentation contribution, which becomes more important at the this low region, might be needed.

¹where R is defined in the (η, ϕ) -plane, $R = \sqrt{\Delta\eta^2 + \Delta\phi^2}$.

²following the approach proposed by [3].

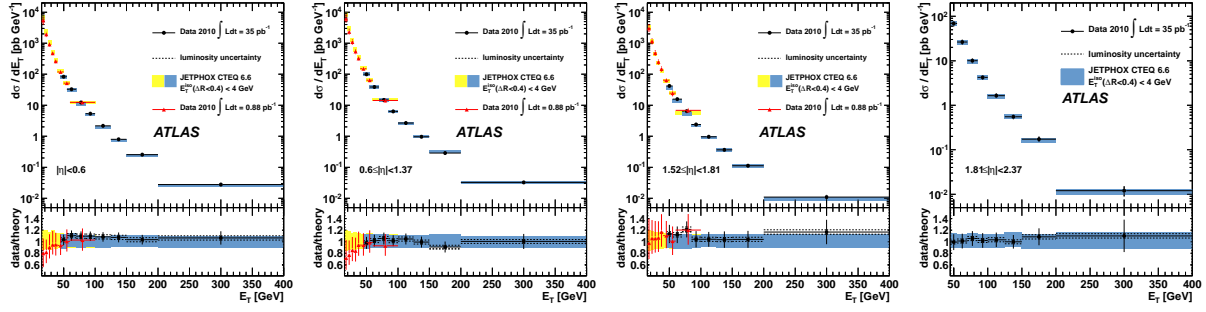


Figure 1: Measured (dots) and expected (shaded area) inclusive prompt photon production cross-section, and their ratio, as a function of the photon E_T and in four different $|\eta|$ regions [3, 4].

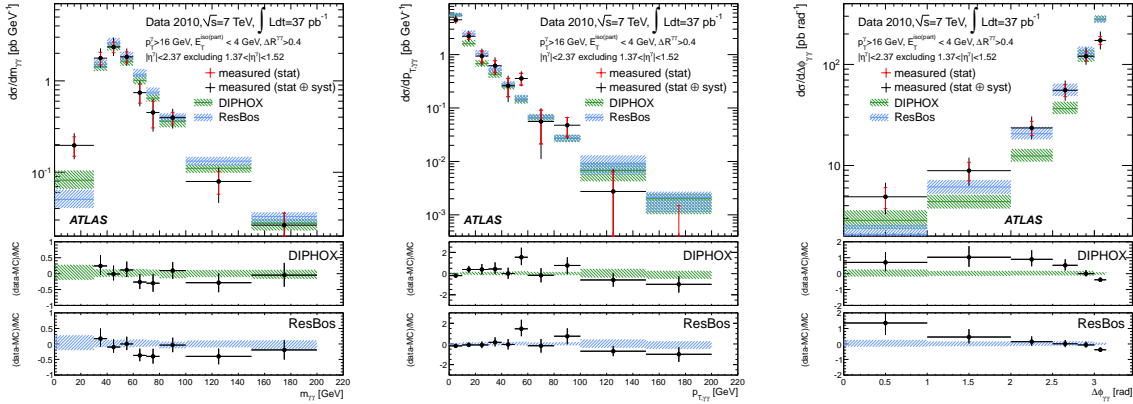


Figure 2: Measured (solid circles) and expected (hatched bands) differential di-photon production cross-sections, and their relative difference, as a function of $m_{\gamma\gamma}$ (left), $p_{T,\gamma\gamma}$ (middle) and $\Delta\phi_{\gamma\gamma}$ (right) [5].

In Fig. 2, the differential cross section for the di-photon production is shown as a function of $m_{\gamma\gamma}$, $p_{T,\gamma\gamma}$ and $\phi_{\gamma\gamma}$. The measurement is compared to NLO computations from DIPHOX[10] and RESBOS[11]. As previously noticed at the Tevatron, the $\Delta\phi_{\gamma\gamma}$ distribution is broader than the theory prediction. A discrepancy at low $m_{\gamma\gamma}$ can be consequently observed. In general, however, a good agreement is observed over the whole kinematic space explored.

References

- [1] Aurenche, P. *et al.* *Nucl. Phys.* **B297** 661 (1988).
- [2] Aurenche, P. *et al.*, *Phys. Rev.* **D39** 3275 (1989).
- [3] ATLAS Collaboration, *Phys. Rev.* **D83** 052005 (2011).
- [4] ATLAS Collaboration, arXiv:hep-ex/1108.0253, (2011). Submitted to PLB.
- [5] ATLAS Collaboration, arXiv:hep-ex/1107.0581, (2011). Submitted to PLB.
- [6] ATLAS Collaboration, *JINST* **3**, S08003 (2008).
- [7] ATLAS Collaboration, ATLAS-PHYS-PUB-2011-007 (2011), <http://cdsweb.cern.ch/record/1345329>.
- [8] M. Cacciari, G. P. Salam and S. Sapeta, *JHEP* **1004**, 065 (2010).
- [9] M. Fontannaz, J. P. Guillet, and G. Heinrich, *Eur. Phys. J.* **C21**, 303-312 (2001).
- [10] T. Binoth, J. P. Guillet, E. Pilon, and M. Werlen, *Eur. Phys. J.* **C16**, 311-330 (2000).
- [11] C. Balazs, E. L. Berger, P. M. Nadolsky, and C. P. Yuan, *Phys. Rev.* **D76**, 013009 (2007).